

Synthesis and characterization of poly(p-phenylenediamine): TiO₂ nanocomposites and investigation of conducting properties for optoelectronic application

S. BARUAH, N. DEVI, A. PUZARI*

Department of Chemistry, National Institute of Technology Nagaland, Chumukedima, Dimapur, Pin: 797103, Nagaland, India

Poly(p-phenylenediamine) is a potential precursor for designing of new materials for optoelectronic application. Synthesis and characterization of poly(p-phenylenediamine) – TiO₂ nanocomposites has been demonstrated. Structural change observed due to the formation of nanocomposites was correlated with concomitant change in conducting behavior of the parent polymer. Polymer nanocomposite was synthesized through an *in-situ* oxidative polymerization technique with simultaneous dispersion of TiO₂ nanoparticles. TiO₂ nanoparticles were synthesized via sol-gel process. Structural characterization was accomplished by using conventional spectroscopic and imaging techniques. I-V measurement of the nanocomposites revealed that the nearly non-conducting poly(p-phenylenediamine) after structural modification exhibits conductivity of 10⁻⁶ S/cm leading to formation of wide band gap semiconducting materials.

Keywords: *poly(p-phenylenediamine); nanocomposite; in-situ polymerization; optoelectronics; semiconductor*

1. Introduction

Use of organic polymers as conductors or semiconductors as a replacement for conventional metals is always of high demand [1]. This is because of the easy processability of polymeric materials which enables one to readily cast such materials as films, foils, and fibers by standardized procedures. Apart from this, low cost and lower weight of such materials are another important aspects [2]. Electrically conducting polymers are used as electrodes [3] or components of batteries [4] as well as construction of solar cells [5]. Even the conductivity of insulating polymers can be sufficiently increased by doping to act as semiconductors [6]. (e.g. iodine, sodium naphthalide, camphorsulphonic acid etc.). In such cases, when the polymer transfers an electron to the dopant to exhibit semiconductor properties it is called a p-type semiconductor (conduction via holes in the valence band) and in the reverse case it is called n-type semiconductor. The most interesting point about polymer doping is that polymer responds to

a wide variety of dopants which enables us to tune the conductivity of polymer to required level.

Poly(p-phenylene)s are relatively stable in air compared to polyacetylenes which exhibit better conducting properties [7]. Poly(p-phenylenediamines) are interesting compounds for designing newer materials for optoelectronic application because of the presence of extensively delocalized conjugation in the polymer structure. Thermal excitation of such molecules promotes some fraction of electrons to higher bonding level which results in changing the conducting behavior. Such polymers are known to exhibit thermoelectric switching behavior [8]. It is therefore anticipated that synthesis of hybrid polymer composites from such polymers will unveil many application prospects in the field of optoelectronics. Encapsulation of nanoparticles in the matrix of polymeric compounds helps tuning the physical characteristics of the resulting nanocomposites through structural engineering. TiO₂ nanoparticle has been successfully used by several researchers for tuning the conducting properties of PANI [9]. Hybrid materials of TiO₂ nanoparticles with PANI were reported in literature [10]. Herein, we

*E-mail: amrit09us@yahoo.com

have reported synthesis and characterization of poly(*p*-phenylenediamine) – TiO₂ nanocomposite and investigation of a change in conducting behavior of the parent polymer due to formation of nanocomposite. Moreover, TiO₂ nanoparticle based composites also exhibit photocatalytic activity [11] and this fact reflects the possibility of using such nanocomposites for various purposes.

TiO₂ nanorods are known to be used for enhancement of efficiency of perovskite solar cells, for development of light emitting devices etc. [12]. In the present study, we have reported structural modification of poly(*p*-phenylenediamine) through incorporation of TiO₂ nanoparticles to obtain hybrid polymer nanocomposites. Structural change observed has been correlated with the change in conducting behavior of the parent polymer. Structural characterization using various sophisticated techniques like FT-IR, FESEM, XRD etc. has also been reported.

2. Experimental

2.1. Materials and methods

Materials used for the synthesis were procured from TCI, Japan and were used as received. Products were characterized by using FT-IR, XRD, FE-SEM, UV-Vis spectroscopy and TGA. FT-IR data were recorded by using single beam Fourier transform infrared spectrometer (Cary 630 FT-IR) at room temperature in the range of 400 cm⁻¹ to 4000 cm⁻¹. For morphological analysis, field emission scanning electron microscopy was used. Carl Zeiss Sigma VP field emission scanning electron microscope (FE-SEM) was used for this purpose. XRD data were recorded on a RIGAKU Ultima IV X-ray diffractometer. The UV-Vis absorption spectra were recorded in the wavelength range of 200 nm to 800 nm using a spectrophotometer (Cary 100 UV-Vis spectrophotometer). Photoluminescence (PL) measurements were carried out in Cary Eclipse fluorescence spectrometer.

2.2. Synthesis

Sol gel method was used for synthesis of titanium dioxide nanoparticles using a standard literature procedure [13]. Synthesis of chloroglycinato 1,10-phenanthroline copper(II) monohydrate was performed by using a literature procedure [14]. Accordingly, 0.249 g (0.001 mol/dm³) of CuSO₄·5H₂O was dissolved in 5.0 mL of 1 mol/L HCl and taken in a test tube. In another test tube, glycine (0.750 g, 0.001 mol/dm³) and phenanthroline (0.198 g, 0.001 mol/dm³) were dissolved in 5.0 mL of 1 mol/L HCl solution. The two solutions were then mixed properly in a 50.0 mL round bottom flask to obtain a blue colored solution. The resulting solution was then stirred continuously for 1 h at 70 °C which resulted in the formation of a green colored precipitate. The precipitate obtained was then filtered and washed with cold water (2 × 5.0 mL) and then dried in the oven at 60 °C for 40 min to obtain a green colored complex. The following literature procedure [15] was employed for synthesis of cis-bisglycinato copper(II) monohydrate. A homogeneous mixture of Cu(OAc)₂·H₂O and glycine was taken in a agate mortar in 1:2 molar ratio and the mixture was ground at room temperature with simultaneous addition of a small amount of solid base NaOH (~1 %). The color of the mixture was changed from green to dark blue in 1 h. Product obtained has washed with little amount of ethanol and cold water and finally dried in vacuum.

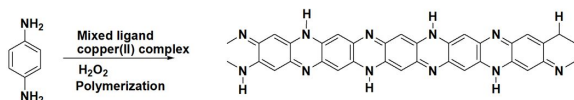
2.2.1. General procedure for synthesis of nanocomposites

6.0 × 10⁻³ mol/dm³ of 1,4 diaminobenzene dihydrochloride was dissolved in 1.5 mL of deionized water and 30 mg (0.0008 mol/dm³ and 0.0013 mol/dm³) of copper (II) complex was added to the solution. The reaction mixture was stirred until the copper(II) complex was completely dissolved. Specific amount of TiO₂ nanoparticles was added to the solution followed by addition of 1.5 mL of 30 % H₂O₂. An instantaneous exothermic reaction took place. The reaction mixture was then stirred continuously at 40 °C for 30 min. The solid product obtained was washed with minimum

amount of deionized water (2×2.0 mL) and finally dried in the oven at 60°C . The following stoichiometric ratio as shown in Table 1 was maintained for synthesis of the four nanocomposites.

3. Results and discussion

Design of polymeric superstructures involving nanomaterials are of key interest for development of materials for electronic application. TiO_2 nanoparticles are important particulate matter for preparation of ordered assemblies of structures from polymeric compounds [16]. Protection of the surface of the nanoparticles by organic molecules influences the process of self-assembly and allows control of chemical functionality of the organic moiety. Hence, it becomes possible to obtain new polymeric super structures with tailor made properties [17]. Therefore, in case of the hybrid polymeric nanocomposites, the ratio of composition of the constituents primarily controls the structural assembly and hence, the collective structural behavior.



Scheme 1. Oligomerization reaction of 1,4-diaminobenzene.

Oxidative polymerization of 1,4-diaminobenzene in presence of copper(II) catalyst (Scheme 1) produces $-\text{C}=\text{N}$ bonded polymer [18]. For synthesis of the polymer nanocomposites, we have used analogous polymerization technique reported in literature for oxidative polymerization of p-phenylenediamine [8], but with simultaneous dispersion of calculated amount of TiO_2 nanoparticles in the reaction mixture. Thus *in-situ* polymerization technique was employed for synthesis of the nanocomposites.

Proton NMR spectrum recorded for the polymer indicates the presence of terminal $-\text{NH}_2$ group in the oligomer. Characteristic peak for the terminal $-\text{NH}_2$ group of the oligomer was obtained at δ 3.2. Aromatic protons of the oligomer show the charac-

teristic peak in δ range of 6.86 ppm to 8.06 ppm. The ^1H NMR spectrum of the oligomer is also indicative of presence of two types of rings in the polymer i.e. quinoid and benzenoid form of benzene. Usually, such type of polymerization process leads to formation of oligomeric products as is indicated from reported value of MALDI mass spectra. Highest m/e value obtained for such polymers is 1470 indicating that 14 units of monomers have combined to form the oligomer [8]. Oligomers derived from diaminobenzene compounds have the capacity to coordinate with metal centers and possess many interesting properties [19].

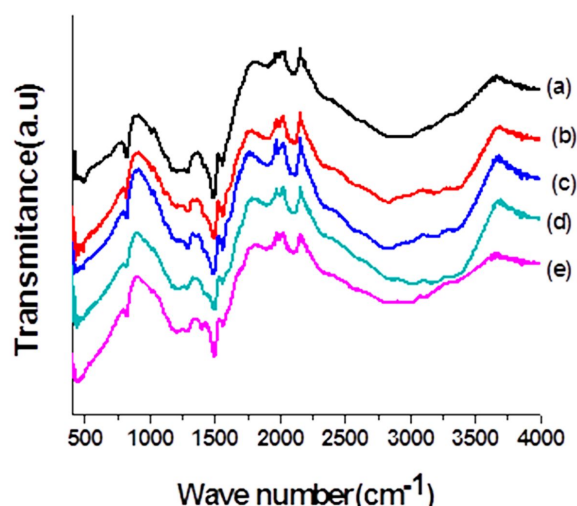


Fig. 1. FT-IR spectra of (a) poly(p-phenylenediamine); (b) nanocomposite - 1; (c) nanocomposite - 2; (d) nanocomposite - 3; (e) nanocomposite - 4.

In case of the polymer nanocomposite, it has been observed that the oligomer effectively coordinates with Ti metal center of TiO_2 nanoparticles. The strong infrared absorption due to $-\text{C}=\text{N}-$ stretching vibrations of the quinonoid, which is reported at 1565 cm^{-1} for poly(p-phenylenediamine), has been found to shift to 1572 cm^{-1} for the nanocomposites which indicates coordination of the $-\text{C}=\text{N}-$ moiety of the oligomer with Ti metal center. $\text{C}=\text{C}$ stretching modes for the benzenoid units occurring at 1490 cm^{-1} for the polymer also shifted to 1509 cm^{-1} in case of the nanocomposite. The bands at 1297 cm^{-1} and 1235 cm^{-1} have been attributed to $\text{C}-\text{N}$

Table 1. Stoichiometric ratio of reactants for synthesis of nanocomposites.

Composite No.	Amount of 1,4-diamino benzene	wt.% of TiO ₂ nanoparticle	Copper complex used	Amount of copper complex
1.	6.0×10^{-3} mol/dm ³	10	Chloro-glycinato 1,10 phenanthroline copper(II) monohydrate	30 mg (0.0008 mol/dm ³)
2.	6.0×10^{-3} mol/dm ³	12	Chloro-glycinato 1,10 phenanthroline copper(II) monohydrate	30 mg (0.0008 mol/dm ³)
3.	6.0×10^{-3} mol/dm ³	10	Cis-bisglycinato copper(II) monohydrate	30 mg (0.0013 mol/dm ³)
4.	6.0×10^{-3} mol/dm ³	12	Cis-bisglycinato copper(II) monohydrate	30 mg (0.0013 mol/dm ³)

stretching mode of benzenoid unit. Further to this, the $-\text{NH}_2$ stretching vibration of parent oligomer which is observed at 3333 cm^{-1} has been shifted for the nanocomposites. The same has been observed at 3125 cm^{-1} , 3153 cm^{-1} , 3113 cm^{-1} and 3116 cm^{-1} , respectively for the four nanocomposites. These findings also reveal that the hydrogen bonding in the polymer complex became stronger after coordinating with TiO₂ nanoparticles [20]. IR spectra of the four nanocomposites along with the IR spectra of poly(p-phenylenediamine) are depicted in Fig. 1.

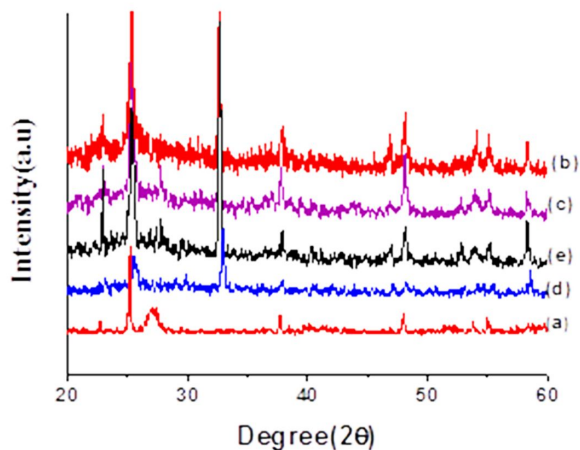


Fig. 2. XRD patterns of (a) TiO₂ nanoparticle; (b) nanocomposite – 1; (c) nanocomposite – 2; (d) nanocomposite – 3; (e) nanocomposite – 4.

Structural investigations like phase identification, crystallinity and crystallite size of the nanocomposites were carried out by powder X-ray

diffraction using secondary monochromator in the range of 2θ from 10° to 80° . Fig. 2 represents the XRD spectra of the four nanocomposites and TiO₂ nanoparticle. From the figure it is clear that for TiO₂ nanoparticle, the diffraction peak corresponds to the anatase phase with good crystalline nature.

The peaks of the samples were identified by comparison with JCPDS Card No. 84-1286. Comparison of 2θ angles confirms the anatase structure of TiO₂ nanoparticles with $2\theta = 25.4^\circ$. The other diffraction peaks at 37.78° , 47.88° , 54.50° and 63.32° can be ascribed to the crystallographic structure of anatase phase. Similarly 32.7° and 58° peaks can be attributed to the semicrystalline form of poly(p-phenylenediamine). The average particle size of the TiO₂ nanoparticles in pure state and in the composites has been calculated by using Scherrer equation. According to Scherrer formula average crystalline size, L is given by:

$$L = K\lambda / \beta \cos \theta \quad (1)$$

where L represents the mean size of the ordered (crystalline) domains, K represents a dimensionless shape factor, with a value close to unity. The shape factor having a typical value of about 0.9 λ represents the X-ray wavelength, β represents the line broadening at half the maximum intensity (FWHM) and θ is the Bragg angle. Average particle size calculated for pure TiO₂ nanoparticle and TiO₂ nanoparticle in the four studied nanocomposites are given in Table 2.

Table 2. Average particle size of TiO₂ nanoparticles in different composites.

S. No.	TiO ₂ nanoparticle	Average particle size [nm]
1	Pure TiO ₂ nanoparticle	43.5
2	TiO ₂ nanoparticle in nanocomposite – 1	38.4
3	TiO ₂ nanoparticle in nanocomposite – 2	36.8
4	TiO ₂ nanoparticle in nanocomposite – 3	36.9
5	TiO ₂ nanoparticle in nanocomposite – 4	34.5

From the table it is apparent that the particle size of pure TiO₂ nanoparticles has decreased in all the four nanocomposites. The decrease in particle size in the nanocomposites can be attributed to the stabilizing factor offered by the anchoring polymer molecules. It is anticipated that coordination of the oligomer with the TiO₂ nanoparticle in the nanocomposite probably influences the aggregation process of TiO₂ nanoparticles, thereby affecting the particle size. It is obvious that the presence of polymer layers on the nanoparticle surface acts as a screening agent that prevents the penetration of the nanoparticles and restricts the growing of the nanoparticles [21]. This size reduction leads to some quantum confinement effect to influence the electrical transport properties of the nanocomposites. However, in case of pure TiO₂ nanoparticles, reduction of particle size leads to an increase in the energy gap and hence, decreases the conductivity through hopping of charge carriers [22]. For the polymer matrix nanocomposites a synergistic effect influences the properties of the nanocomposites as the properties are collectively influenced by polymer matrix and the inorganic nanoparticle. Due to the quantum confinement effect referred above, we have observed improvement in the conducting behavior of the nanocomposites compared to that of the parent polymer, poly-(p-phenylenediamine). Reported conductivity of poly(p-phenylenediamine) is 2.4×10^{-10} S/cm, i.e. the polymer is nearly nonconducting [23], while observed conductivities of the nanocomposites are of the order of 10^{-6} S/cm (Table 3). Therefore, the work presented here demonstrates efficient techniques to synthesize poly(p-phenylenediamine) nanocomposites with TiO₂ nanoparticles which exhibit interesting

conducting behavior, suitable for application in optoelectronics.

Field emission scanning electron microscope (FE-SEM) was used for morphological study of the nanocomposites. As representative case for two different types of nanocomposites involving two different copper complexes, we have recorded the FE-SEM images for nanocomposite – 1 and nanocomposite – 4. FE-SEM images recorded for the samples are shown in Fig. 3.

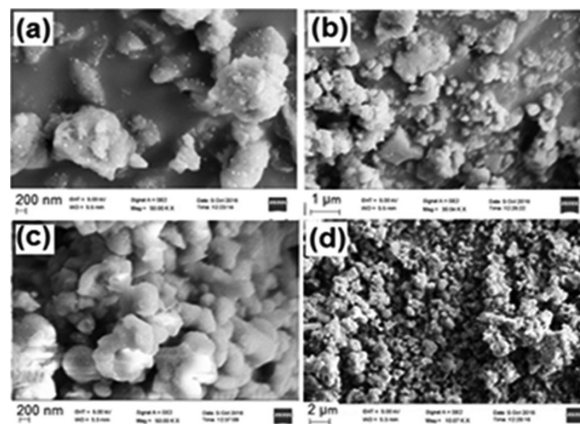


Fig. 3. FE-SEM images of (a) nanocomposite – 1 (scale bar 200 nm); (b) nanocomposite – 1 (scale bar 1 μm); (c) nanocomposite – 4 (scale bar 200 nm); (d) nanocomposite – 4 (scale bar 1 μm).

Agglomeration of TiO₂ nanoparticles in the nanocomposites in globular form has been observed in the FE-SEM images. The images also reflect semi-crystalline nature of the nanocomposites. With an increase in amount of TiO₂ nanoparticles a subsequent increase in the agglomerated grains was found in the nanocomposite. It has been observed

that morphology of the nanocomposites is compact and nonporous.

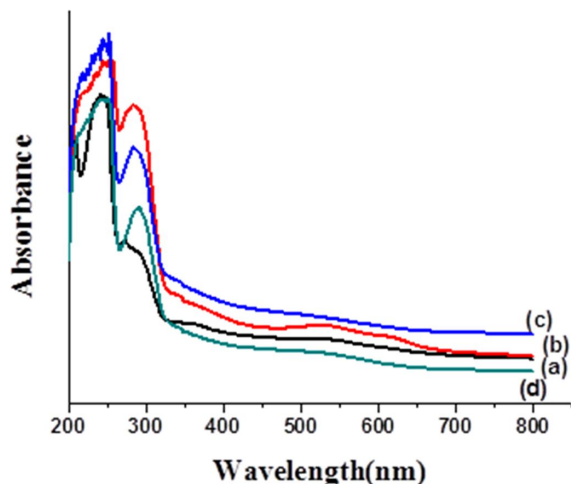


Fig. 4. UV-Vis spectra of the nanocomposites (a) TiO₂ nanoparticle; (b) nanocomposite – 1; (c) nanocomposite – 2; (d) nanocomposite – 3; (e) nanocomposite – 4.

UV-Vis absorption and PL emission characteristics of the nanocomposites exhibit characteristic energy gap that conforms with anatase TiO₂. UV-Vis spectra of the nanocomposites show a strong absorption peak due to TiO₂ nanoparticle at 285 nm, corresponding to band gap energy of 3.77 eV. Band gap is calculated by using the formula:

$$E = h \cdot c / \lambda \quad (2)$$

where E corresponds to band gap energy, λ corresponds to cut off wavelength (found to be 330.0 nm from Fig. 4), h is the Planck's constant and c the velocity of light. The value indicates that the nanocomposites can be categorized as wide band gap semiconductors (WBGs). Compared to conventional semiconductors, WBGs are convenient to use in devices that operate at higher voltages, frequencies and temperatures. The semiconductor band gap energy of crystalline bulk anatase is 3.25 eV [24]. Wide band gap materials have the band gap of the order of 2 eV to 4 eV [25]. Apart from that appearance of visible light absorption, the tail portion of the UV-Vis spectrum indicates the

presence of oxygen vacancy states between the valence and conduction bands in the TiO₂ band structure. UV-Vis spectra of the four nanocomposites in methanol solvent are shown in Fig. 4.

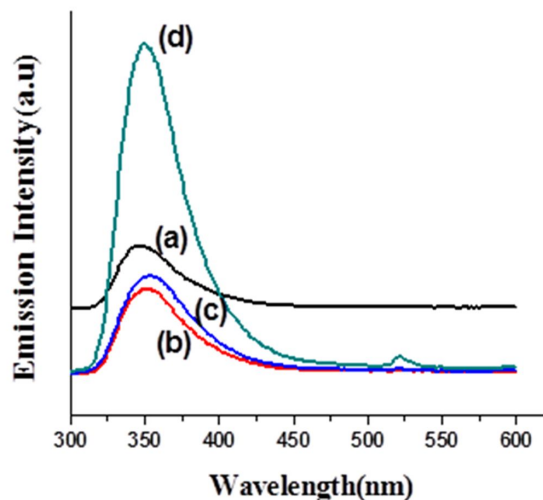


Fig. 5. Photoluminescence (PL) spectra of four *p*-phenylenediamine nanocomposites (a) nanocomposite – 1; (b) nanocomposite – 2; (c) nanocomposite – 3; (d) nanocomposite – 4.

Photoluminescence (PL) signal gives an idea about recombination of photoinduced electrons and holes. Surface structure and oxygen defects of TiO₂ nanoparticles influence the PL signals. The PL emission spectra of the nanocomposites (Fig. 5) are very broad and show no clear structure.

Hence, these spectra can be attributed to oxygen vacancy states, whose energy levels are 1 eV below the lower end of the conduction band. Depending on experimental conditions, different degrees of oxygen vacancies can be formed, which is reflected in PL spectra [26]. From the figure we can also infer that nanocomposite – 2 and nanocomposite – 4 have higher luminescence efficiency than nanocomposite – 1 and nanocomposite – 3 as they have more anatase TiO₂ particles. This can be explained by charge transfer mechanism [27].

Thermogravimetric analysis of the samples was carried out to study thermal stability of the nanocomposites. The thermograms of the nanocomposites are shown in Fig. 6. For all the four nanocomposites, initial weight loss of 6 % to

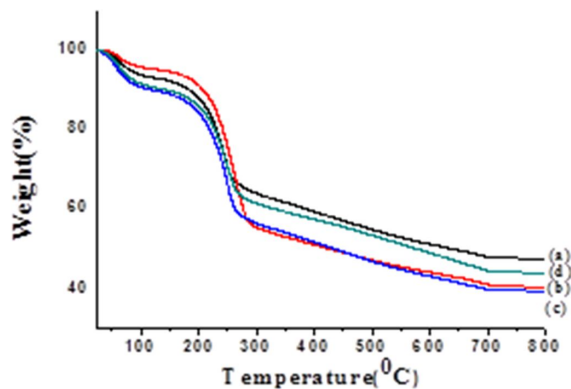


Fig. 6. TGA spectrum of four p-phenylenediamine nanocomposites (a) nanocomposite – 1; (b) nanocomposite – 2; (c) nanocomposite – 3; (d) nanocomposite – 4.

8 % was recorded up to a temperature of 100 °C. This can be attributed to the loss of moisture content in the nanocomposites. Beyond that temperature, the nanocomposites are thermally stable up to a temperature of 150 °C beyond which they start decaying slowly. From 200 °C onwards the nanocomposites decay continuously in two steps. 30 % to 40 % weight loss was recorded for all the nanocomposites up to a temperature of 280 °C. This indicates degradation of the polymeric structure.

Properties of polymer nanocomposite materials can be drastically tuned through appropriate use of nanofillers like SiO₂, TiO₂ etc. Apparently, the conduction behavior of the nanocomposites can be tuned by using such nanofillers, which has been observed in the reported case. The current vs. voltage characteristics of the nanocomposites exhibit nearly nonlinear character (Fig. 7).

Polymers like LDPE (low density polyethylene), HDPE (high density polyethylene), when filled with ZnO microparticles exhibit varistor effect [28]. Conducting polymer/CNT nanocomposites are used as electrochemical electrodes due to their high conductivity and stability [29]. Such nanocomposites can be effective probes for detection and immobilization of biomolecules due to the fact that CNT can promote electron transfer reactions in proteins and enzymes [30]. There

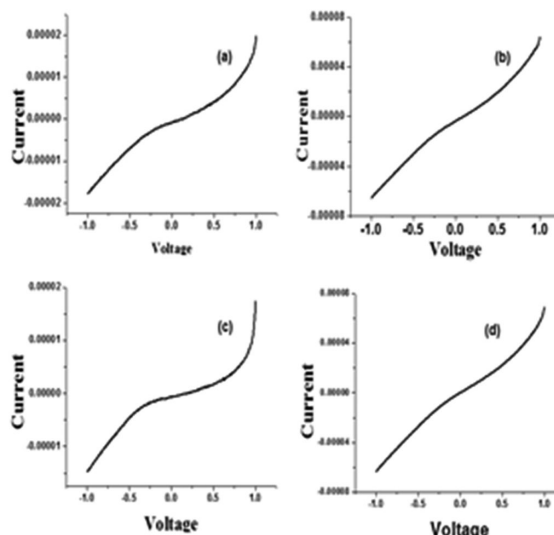


Fig. 7. Current vs. voltage curves for the four nanocomposites (a) nanocomposite – 1; (b) nanocomposite – 2; (c) nanocomposite – 3; (d) nanocomposite – 4.

are some other benefits associated with nonlinear characteristics of polymeric nanocomposites like self-heating behavior [31] and photoconductivity [32]. Self-heating behavior of such polymer nanocomposites is useful for making current limiting switches. This fact highlights the importance of such nanocomposites in technological sector.

Table 3. Conductivity of the nanocomposites.

Nanocomposite	Resistivity [Ω·cm]	Conductivity [S/cm]
Nanocomposite – 1	5.197×10^5	1.926×10^{-6}
Nanocomposite – 2	2.035×10^5	4.914×10^{-6}
Nanocomposite – 3	9.312×10^5	1.074×10^{-6}
Nanocomposite – 4	2.711×10^5	3.685×10^{-6}

Using the current-voltage (I-V) curve, the resistivity (ρ) of the nanocomposites has been calculated from the values of the parameters, like resistance (R), area of the pellet (A) and thickness of the pellet (l) used during I-V measurement. The resistivity for the four different nanocomposites have been calculated from the relation:

$$\rho = (A/l)R_b \quad (3)$$

where ρ is the resistivity, l is the thickness of the pellet, A represents area of the pellet and R_b is the bulk resistance of the pellet. The resistivity value can be used to calculate the conductivity (σ) of the nanocomposites. The resistivity and conductivity values calculated for the nanocomposites are tabulated in Table 3.

The conductivity (σ) of semiconducting materials usually falls in the range between 10^{-8} S/cm to 10^3 S/cm and the resistivity (ρ) values for semiconducting materials fall within the range 10^8 Ω -cm to 10^{-3} Ω -cm. Therefore, apparently the conductivity as well as resistivity values of the nanocomposites fall well within the range of the values for semiconducting materials. It is to be noted that reported value of conductivity for protonated form of poly-(p-phenylenediamine) is 2.4×10^{-10} S/cm, i.e. the polymer is nearly nonconducting [33]. This fact indicates that encapsulation of TiO₂ nanoparticles in the polymer matrix has influenced the structural organization of the polymer because of which, the conductivity values have been drastically improved. Coordination ability of the –C=N– bonded oligomers enables structural reorganization of the nanocomposite framework leading to a well ordered structure with inclusion of TiO₂ nanoparticles, which eventually changes the electron population as well as the band gap. From the table it has also been observed that conductivity value increases with an increase in concentration of TiO₂ nanoparticles.

4. Conclusion

We have successfully demonstrated synthesis and characterization of poly(p-phenylenediamine) – TiO₂ nanocomposites. Incorporation of TiO₂ nanoparticles into the polymer matrix resulted in significant change in conducting properties of the parent polymer. Nearly non conducting poly(p-phenylenediamine) has been converted to semicrystalline wide band gap semiconducting nanocomposites which has potential utility for use in devices that operate at higher voltages. In general, it can be stated that the materials developed will have significant utility in the field of optoelectronics.

Acknowledgements

The author sincerely acknowledges the Department of Science and Technology, Government of India, for financial support received under Project Grant (Project ID: INT/RUS/RFBR/P-221).

References

- [1] TROISI A., *Nature. Mat.*, 8 (2009), 538.
- [2] PAINTER P. C., COLEMAN M. M., *Tech. Pub. CO Lan. PA.*, (1997).
- [3] NAEGELE D., BITTHN R., *Solid. State. Ionics*, 28 (1988), 983.
- [4] MUENCH S., WILD A., FRIEBE C., HÄUPLER B., JANOSCHKA T., SCHUBERT U.S., *Chem. Rev.*, 116 (16) (2016), 9438.
- [5] (a) BLANKENBURG L., SENSFUSS S., SCHACHE H., MARTEN J., MILKER R., SCHRODNER M., *Synth.Met.*, 199 (2015), 93. (b) BENANTI T.L., VENKATARAMAN D., *Photosynth. Res.*, 87 (2006), 73.
- [6] BAKHSHI A.K., VALLA G., *Mater. J. Sci. Ind. Res.*, 63 (2004), 715.
- [7] KOVACIC P., JONES M. B., *Chem. Rev.*, 87 (2) (1987), 357.
- [8] PUZARI A., BARUAH J. B., *React. Funct. Polym.*, 47 (2001), 147.
- [9] (a) XU J.C., LIU W.M., LI H.L., *Mater. Sci. Eng.*, 25 (4) (2005), 444. (b) ARORA R., MANDAL U.K., SHARMA P., SRIVASTAV A., *Mater. Today Proc.*, 2 (2015), 2767.
- [10] (a) AVU A., OK A., *Synth. Met.*, 157(2007), 235. (b) GANESAN R., GEDANKEN A., *Nanotech.*, 19 (43) (2008), 435709. (c) GANGOPADHYAY R., DE A., GHOSH G., *Synth. Met.*, 123 (2001), 21.
- [11] SONG Y., ZHANG J., YANG L., CAO S., YANG H., ZHANG J., JIANG L., DAN Y., RENDU P.L., NGUYEN T.P., *Mater. Sci. Semicond. Proc.*, 42 (1) (2016), 54.
- [12] (a) ZHANG Z.L., LI J.F., WANG X.L., QIN J.Q., SHI W.J., LIU Y.F., GAO H.P., MAO L., *Nanoscale. Res. Let.*, 12 (2017), 43. (b) TSAI T.Y., YAN P.R., YANG S.H., *Nanoscale Res. Let.*, 11 (2016), 516.
- [13] PERUMAL S., SAMBANDAM C.G., PRABU K. M., ANANTHAKUMAR S., *Int. J. Res. Eng. Tech.*, 3 (4) (2014), 651.
- [14] BARUAH S., PUZARI A., *Inorg. Nano. Met. Chem.*, 47 (11) (2017), 1542.
- [15] CHEN T., LIANG B., XIN X., *J. Phys. Chem. Solid.*, 58 (1997), 951.
- [16] SANG L., ZHAO Y., BURDA C., *Chem. Rev.*, 114 (19) (2014), 9283.
- [17] TAO P., LI Y., RUNGTA A., VISWANATH A., GAO J., BENICEWICZ B. C., SIEGELA R. W., SCHADLER L.S., *J. Mater. Chem.*, 21 (2011), 18623.
- [18] CATALDO F., *Eur. Polym. J.*, 32 (1) (1996), 43.
- [19] MEDEROS A., DOMINGUEZ S., HERNANDEZ-MOLINA R., SAN-CHIZ J., BRITO F., *Coord. Chem.Rev.*, 195 (1999), 857.
- [20] ZHANG L., LIU P., SU Z., *Polym. Degrad. Stab.*, 91 (2006), 2213.

- [21] KUTVONEN A., ROSSI G., PUISTO S.R., ROSTEDT N.K.J., NISSILA T.A., *J. Chem Phys.*, 137 (2012), 901.
- [22] AVINASH B.S., CHATURMUKHA V.S., JAYANNA H.S., NAVEEN C.S., RAJEEVA M.P., HARISH B.M., SURESH S., LAMANI R., *AIP Conf. Proc.*, 1728 (2016), 20426.
- [23] NAKAMURA J., NEGISHI N., KUTSUNA S., IHARA T., SUGIHARA S., TAKEUCHI K., *J. Mol. Catal.*, 161 (2000), 205.
- [24] YOSHIKAWA A., MATSUNAMI H., NANISHI Y., *Wide Bandgap Semiconductors. Springer*, 2 (2007).
- [25] LIU B., WEN L., ZHAO X., *Mater. Chem. Phys.*, 106 (2007), 350.
- [26] LIQIANG J., YICHUN Q., BAIQI W., SHUDAN L., BAOJIANG J., LIBIN Y., WEI F., HONGGANG F., JIAZHONG S., *Sol. Energy Mater. Sol. C.*, 90 (2006), 1773.
- [27] ABAZOVIC N.D., COMOR M.I., DRAMICANIN M.D., JOVANOVIC D.J., AHRENKIEL S.P., NEDELJKOVIC J.M., *J. Phy. Chem. B.*, 110 (50) (2006), 25366.
- [28] LIN C.C., LEE W.S., SUN C.C., WHU W.I.I., *Ceram. Int.*, 34 (2008), 131.
- [29] PENG C., ZHANG S., JEWELL D., CHEN G.Z., *Prog. Nat. Sci.*, 18 (7) (2008), 777.
- [30] (a) YANG T., ZHOU N., ZHANG Y., ZHANG W., JIAO K., LI G., *Biosens. Bioelectron.*, 24 (2009), 216. (b) KORKUT S., KESKINLER B., ERHAN E., *Talanta.*, 76 (2008), 1147.
- [31] AZULAY D., FYLON M., ESHKENAZI Q., TOKER D., BALBERG M., SHIMONI N., MILLO O., BALBERG I., *Phys. Rev. Lett.*, 90 (2003), 23660.
- [32] NIKOLAEVA E.V., OZERIN S.A., GRIGORIEV E.I., CHVALUN S.N., GERASIMOV G.N., TRAKHTENBERG L.I., *Mater. Sci. Eng. C.*, 8 (1999), 217.
- [33] TRLICA J., SAHA P., QUADRAT O., STEJSKAL J., *Physica A*, 283 (2000), 337.

Received 2017-11-23

Accepted 2019-03-01